J of Nuclear Medicine Technology, first published online May 12, 2011 as doi:10.2967/jnmt.111.087445

# $^{99m}$Tc-Based Imaging of Transplanted Neural Stem Cells and Progenitor Cells

Jacqueline A. Gleave[1], John F. Valliant[2,3], and Laurie C. Doering[1]

*[1]Pathology and Molecular Medicine, McMaster University, Hamilton, Ontario, Canada; [2]Department of Chemistry, McMaster University, Hamilton, Ontario, Canada; and [3]Department of Medical Physics and Applied Radiation Sciences, McMaster University, Hamilton, Ontario, Canada*

Cell therapy for neurologic disorders will benefit significantly from progress in methods of noninvasively imaging cell transplants. The success of current cell therapy has varied, in part because of differences in cell sources, differences in transplantation procedures, and lack of understanding of cell fate after transplantation. Standardization of transplantation procedures will progress with noninvasive imaging. In turn, in vivo imaging will enhance our understanding of neural transplant biology and improve therapeutic outcomes. The goal of this study was to determine the effect of a $^{99m}$Tc-based probe on neural stem and progenitor cell transplants and validate the SPECT images of the transplanted cells. **Methods:** We previously developed a method to label neural stem and progenitor cells with $^{99m}$Tc to visualize these cells in the brain with SPECT. The cells were initially labeled with a permeation peptide carrying a chelate for $^{99m}$Tc. The proliferation and differentiation characteristics of the labeled cells were studied in tissue culture. In parallel experiments, the labeled cells were stereotactically injected into the rat brain, and the site of transplantation was verified with histochemistry and phosphorimaging. **Results:** The accuracy of the transplant location obtained by SPECT was confirmed by comparison with phosphorimages and histologic sections of the brain. The labeling did, however, decrease the proliferative capacity of the neural stem and progenitor cells. **Conclusion:** The labeling technique described here can be used to standardize the location of cell transplants in the brain and quantify the number of transplanted cells. However, a $^{99m}$Tc-based probe can decrease the cellular proliferation of neural progenitor cells.

**Key Words:** SPECT/CT; neural stem/progenitor cells; technetium; proliferation; differentiation

**J Nucl Med Technol 2011; 39:114–120**
DOI: 10.2967/jnmt.111.087445

Stem cell therapy is considered to be a promising treatment option for several neurologic disorders. Transplantation of neural stem and progenitor cells (NSPCs) in the damaged brain is being evaluated for the treatment of Parkinson disease (PD), Alzheimer disease, Huntington disease, traumatic brain injury, and spinal cord injury (*1–5*). NSPCs are capable of self-renewal and differentiation into the 3 main cell lineages of the central nervous system: astrocytes, oligodendrocytes, and neurons (*6*). NSPCs can be isolated from fetal, embryonic, and adult brain sources and can be expanded in vitro as heterogeneous aggregates of cells termed neurospheres. The properties of NSPCs make them an attractive therapeutic option for neurologic disorders.

Stem cell therapy in animal models of PD has produced variable outcomes. One study demonstrated that embryonic stem cells could be used to successfully treat PD; however, 40% of these animals had teratoma formation (*7*). Studies with adult progenitor cells have shown that although there is graft survival, functional recovery is not consistent (*8*). In contrast, other reports have successfully demonstrated graft survival with the expression of tyrosine hydroxylase, the rate-limiting enzyme in dopamine production, and corresponding functional improvements (*9*). However, in clinical trials of PD, there has been limited success with transplantation therapy (*10,11*). At this time, cell transplantation therapy is highly variable, in part because of difficulties in achieving reproducible cell grafts.

It is important to understand conditions that affect transplant survival and cell fate to decrease the variability observed in transplantation experiments. Molecular imaging techniques can provide valuable information about transplant variables that will enhance transplantation outcomes. There is a need to standardize transplantation procedures using short-term assessment methods and to understand the fate of the transplanted cells using long-term tracking studies.

A previous study found that despite the use of ultrasound-guided injection and highly trained personnel, cell placement was performed correctly only approximately 50% of the time (*12*). The number of transplanted cells has been shown to affect therapeutic outcome (*13,14*). The number of cells transplanted can, in theory, be determined with good accuracy using nuclear imaging methods, including SPECT and the appropriate molecular imaging probe. The ability to determine the number of cells injected into

Received Jan. 5, 2011; revision accepted Mar. 18, 2011.
For correspondence or reprints contact: Laurie C. Doering, McMaster University, 1200 Main St. W., Hamilton, ON L8N3Z5, Canada.
E-mail: doering@mcmaster.ca

the host offers key quantitative and qualitative information about the transplant that in turn will improve the standardization of surgical procedures and allow for greater experimental control in preclinical and clinical studies. The number of cells transplanted can, in theory, be determined, and the number of cells injected into the host offers key quantitative and qualitative information about the transplant that in turn will improve routine procedures. The development of imaging techniques to visualize cell transplants accurately is necessary to standardize grafting techniques and gain greater experimental control in preclinical and clinical studies.

Tat-based peptides are useful tools for incorporating radiolabels, fluorescent protein, or MRI contrast agents into cells (*15–19*). When coupled to $^{99m}$Tc, cells can be labeled with a relatively inexpensive and widely available radionuclide, the short-term shutdown of the Chalk River reactor notwithstanding. $^{99m}$Tc has a half-life of approximately 6 h and decays with an emission of 140-keV γ-rays. These are optimal physical characteristics for γ-camera imaging, and this isotope imparts a low dose-burden to patients (*20*). We have previously shown that we can label a chelate-derived version of a permeation peptide and use it to monitor preliminary transplants (*21*). An initial study of $^{99m}$Tc-labeled cells found no significant effects of the probe on DNA damage or the viability of NSPCs. The aim of this study was to validate the correlation of imaging results with histochemistry and to assess the effect of the probe on cell proliferation and differentiation to determine whether this label is suitable for imaging cell transplants.

## MATERIALS AND METHODS

### Maintenance of Animal Colonies

All animal experiments were performed in accordance with the guidelines specified by the Canadian Council on Animal Care and were approved by the Animal Research Ethics Board of McMaster University.

### High-Performance Liquid Chromatography (HPLC)

Analytic HPLC was performed using a Pursuit C18 5-μm, 2.4-mm MetaGuard column (Varian) and a C18 column (4.6 × 250 mm; Varian). For the mobile phase, solvent A was $H_2O$ containing 20 mM triethylamine (adjusted to pH 3 with trifluoroacetic acid [TFA]), and solvent B was acetonitrile containing 20 mM triethylamine (adjusted to pH 3 with TFA). The elution protocol consisted of a gradient running from 90% solution A and 10% solution B to 10% solution A and 90% solution B over 20 min. The flow rate was 1.0 mL min$^{-1}$, and all runs were monitored at $\lambda = 254$ nm.

Semipreparative HPLC was performed using a C-18 3-μm Luna semipreparative column (150 × 10 mm; Phenomenex). Solvent A was $H_2O$ containing 0.05% TFA, solvent B was acetonitrile containing 0.05% TFA, and the gradient was run using the same protocol as for analytic HPLC. The flow rate was 4.0 mL min$^{-1}$, and the runs were monitored at $\lambda = 254$ nm.

### Solid-Phase Peptide Synthesis

Solid-phase peptide synthesis was performed as previously described (*21*). Briefly, peptides were made on a Fmoc-glycine–loaded Wang resin and, after completion, were cleaved from the resin using a TFA mixture containing 2% 1,2-ethanedithiol, 2% water, and 2% triisopropylsilane. Peptides were lyophilized to yield the peptide and the corresponding rhenium standard.

### Preparation of $^{99m}$Tc Probe

Preparation of the probe was based on a previously described procedure (*21*). For peptide labeling, 4.0 mg ($2.1 \times 10^{-6}$ mol) of the peptide in 200 μL of distilled deionized water were added to the $^{99m}$Tc solution. The reaction was heated in a microwave at 120°C for 5 min. The solvent was removed using a V10 evaporation system (Biotage Inc.), and the crude product was redissolved in 0.5 mL of distilled $H_2O$ using the V10 system. The crude reaction was purified using semipreparative HPLC, and radiochemical purity (98%) was determined using analytic γ-HPLC.

### Preparation of Neurospheres

Neurospheres were prepared as previously described (*21*). Briefly, NSPCs were harvested from 1- to 3-d-old pups. The cells were cultured as neurospheres and used for subsequent experiments between the first and fifth passages.

### Labeling of Dissociated Neurospheres with $^{99m}$Tc Probe

Neurospheres were dissociated using TrypLE Express (Invitrogen). The resulting cell pellet was resuspended in serum-free medium. The cell counts were determined using trypan blue exclusion dye. Cells were plated in tissue culture dishes at a concentration of 10,000 cells/mL. The cells were incubated with 27.3 pmol (592 MBq) of $^{99m}$Tc in 0.01 M phosphate-buffered saline at 37°C for 20 min in a 95% $O_2$, 5% $CO_2$, incubator. The labeled cells were washed and resuspended in the appropriate amount of medium for the subsequent experiments. Labeling efficiency was determined using a dose calibrator that had been calibrated using a National Institute of Standards and Technology–traceable standard and reference standards over a range of activities. Control cells were prepared in an identical manner using 0.01 M phosphate-buffered saline in place of the $^{99m}$Tc probe. For some experiments, a portion of the labeled cells was coincubated with cell-tracker orange (Molecular Probes) according to the manufacturer's instructions to label the cells for identification by fluorescence microscopy.

### Proliferation of Labeled NSPCs

Cells were labeled with $^{99m}$Tc, 27.3 pmol of rhenium standard, or peptide as described previously (*22*). Control cells were labeled with an equal volume of 0.01 M phosphate-buffered saline for 20 min. Proliferation was monitored using a BrdU Cell Proliferation Assay (Chemicon International) according to the manufacturer's instructions.

### Differentiation of Labeled NSPCs

After labeling with the $^{99m}$Tc probe, 27.3 pmol of rhenium, or peptide, the cells were plated onto coverslips coated with poly-L-lysine (Sigma) and laminin (Invitrogen) in a 1:1 ratio of serum-free medium to serum-free medium without epidermal growth factor (Sigma), fibroblast growth factor 2 (Sigma), and heparin (Sigma) containing 1.0% fetal bovine serum (Biowest). The cells were differentiated for 10 d at 37°C in 95% $O_2$ and 5% $CO_2$. The cells were then fixed in acetone, and cell differentiation was assessed using immunocytochemistry. The neuronal and glial phenotypes were identified using monoclonal anti-βIII-tubulin (1:1,000; Promega) and polyclonal anti–glial fibrillary acidic protein (1:100; Dako), respectively. Secondary antibodies included donkey anti-mouse AlexaFluor 594 (1:1,500; Invitrogen) and goat anti-rabbit fluorescein isothiocyanate (1:100; Cedarlane).

### NSPC Transplantation

Three-month-old Sprague Dawley rats were anesthetized by the gaseous anesthetic isoflurane (2.5%–3.0%). Buprenorphine in sterile saline was injected subcutaneously as an analgesic. Rats were placed in a stereotactic apparatus (David Kopf Instruments) in preparation for surgery. A second analgesic, lidocaine, was applied topically on the surface of the scalp before the incision. An incision was made along the top of the skull, and the overlying muscle was scraped away from the skull surface. At the coordinates given below (from Bregma and the dura mater), a dremel drill was used to make a small hole through the skull. The cells were transplanted with a 10-μL Hamilton syringe lowered into the striatum of the rats (from Bregma and the dura anteroposteriorly, mediolaterally, and dorsoventrally, 3 μL were injected at –1.0, −3.0, and −4.0 mm, respectively [nose bar = 0 mm]). The syringe was left in place for 10 min and then slowly removed. The incision was closed with 4-0 silk sutures, and the rat was allowed to recover from the anesthetic.

### SPECT of Cell Transplants

The rats were anesthetized using isoflurane (2.5%–3.0%). SPECT images were acquired using an X-SPECT system (Gamma Medica-Ideas) and a high-resolution parallel-hole collimator followed by a CT scan. The dual-head SPECT/CT system has a SPECT field of view of 10 × 10 cm with a spatial resolution of 2–3 mm. The γ-cameras were fitted with low-energy, high-resolution parallel-hole collimators. One rotation was acquired over 64 projections at 100 s/projection.

SPECT images were reconstructed using iterative ordered-subsets expectation maximization with detector response compensation. In total, 2 iterations with 8 subsets were used, and the reconstructed images were processed with a 3-dimensional gaussian filter of 2 mm in full width at half maximum. Analysis was done by drawing a 3-dimensional region of interest around the cell transplant using AMIDE software (version 0.9.1; http://amide.sourceforge.net). The mean counts were obtained and compared with a calibration curve.

The CT component of the X-SPECT system, which has a flat-panel-detector field of view of 10 × 10 cm, was used for anatomic coregistration. CT information was acquired using 75-kVp x-rays and a tube current of 265 μA with a spot size of 50 μm. Over 360°, 512 projections were acquired, and they were processed with a modified Feldkamp cone-beam reconstruction (version 6.0; Cobra-Exxim). The resulting image had a matrix of 512 × 512 × 512 and a reconstructed voxel size of 155 μm.

### Phosphorimaging of Dissected Rat Brains

Immediately after imaging, the rat was sacrificed and the brain was removed, flash-frozen, and cut into 20-μm sections with a cryostat. The sections were exposed to phosphorimaging film for 15 min and developed using a Storm 840 phosphorimager and ImageQuant TL (GE Healthcare).

### Statistics

The data are presented as mean ± SEM. Statistical analysis was performed using 1-way or 2-way ANOVA with a post hoc Tukey test or a *t* test using Prism software (version 5; GraphPad). Significance is expressed with a confidence interval of $P < 0.05$.

## RESULTS

### Proliferation of Labeled NSPCs

The proliferation of NSPCs after labeling was assessed using the BrdU cell proliferation assay. Labeled cells were incubated with the BrdU reagent for 24 h at 37°C and analyzed in parallel with the control cells. This assay assesses the amount of BrdU incorporated into newly synthesized DNA and is directly proportional to the number of cells that have divided within the 24-h period. $^{99m}$Tc-, rhenium-, or peptide-labeled NSPC proliferation was normalized to control cells that had been incubated with an equal volume of 0.01 M phosphate-buffered saline. This accounts for differences in the primary cells and the age of the cells, because the age of the cells can affect their proliferative ability (*22*). The proliferative abilities of rhenium- and peptide-labeled cells did not significantly differ from one another (103.4% ± 7.8% and 108.5% ± 21.2%, respectively) (Fig. 1). $^{99m}$Tc-labeled cells showed a significant decrease in proliferation (25.4% ± 13.1%) compared with rhenium- and peptide-labeled cells (Fig. 1), indicating that the difference in proliferation was most likely caused by $^{99m}$Tc rather than the peptide itself. [**Fig. 1**]

### Differentiation of Labeled NSPCs

NSPCs isolated from wild-type mouse pups were labeled with $^{99m}$Tc, rhenium, and peptide. Labeled cells were differentiated for 10 d in medium containing 1.0% fetal bovine serum and depleted of growth factors. The percentages of neuronal and glial cells were expressed as a percentage of the total cell number determined by 4′6′-diamidino-2-phenylindole staining of the nuclei. $^{99m}$Tc-, rhenium-, and peptide-labeled cells were normalized to control cells

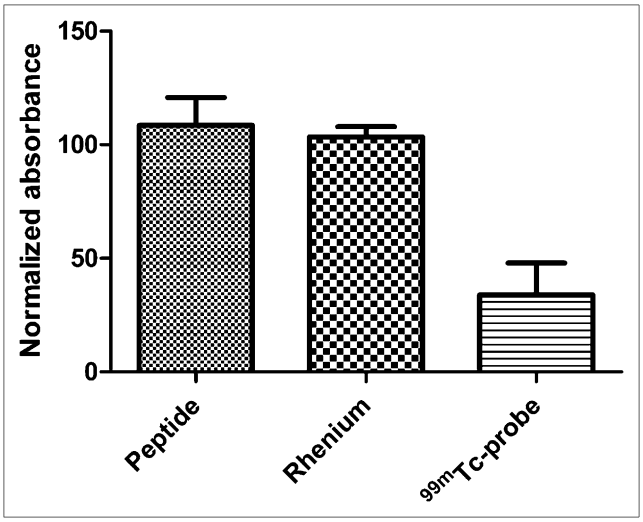


**FIGURE 1.** Cell proliferation assessed by BrdU assay. No significant difference is seen between proliferation of cells labeled with rhenium and peptide. Proliferation of cells labeled with $^{99m}$Tc shows a significant decrease ($P < 0.05$, $n = 3$).

to account for any differences in the cell population due to differences in passage number. The cells labeled with $^{99m}$Tc showed variability in the percentage that differentiated into neurons. Equally, there was variability in the percentage of cells that differentiated into neurons in the control group as well. A greater number of NSPCs in the $^{99m}$Tc-labeled group than in the control group differentiated into neurons. Representative images of labeled neurons and astrocytes [**Fig. 2**] are shown in Figures 2B–2D.

When cell differentiation was compared between the $^{99m}$Tc, rhenium, and peptide groups, a trend toward increased neuronal differentiation was found in both the $^{99m}$Tc and rhenium groups, with the former showing the greatest neuronal differentiation. However, because of the variability in cell differentiation, this trend did not reach significance (Fig. 2A).

### SPECT of Cell Transplants

To determine whether the SPECT images accurately illustrate the location of transplanted NSPCs, in vivo and ex vivo imaging studies were performed using complementary cell labels. Rats were transplanted with $^{99m}$Tc-labeled NSPCs or NSPCs double-labeled with cell-tracker orange (a lipophilic dye) and $^{99m}$Tc. Immediately after surgery, a SPECT/CT image was acquired, the rats were euthanized, and the brains were flash frozen for histology or phosphorimaging to confirm that the SPECT images corresponded to the transplanted cells (Fig. 3). The SPECT image and the [**Fig. 3**] phosphorimage demonstrate the specificity of the activity to the area of the transplanted cells (Figs. 3A–3D). As further confirmation, NSPCs double-labeled with cell-tracker orange and $^{99m}$Tc were transplanted into the forebrain. The SPECT findings correlated with the location of the cells on histology (Figs. 3E–3J).

## DISCUSSION

$^{99m}$Tc is the most widely used radionuclide in diagnostic medicine. It has a reasonably long half-life (6 h) and is readily available in most hospitals, making $^{99m}$Tc-based cell labeling agents accessible to the research community at a reasonable cost. This consideration is important in view

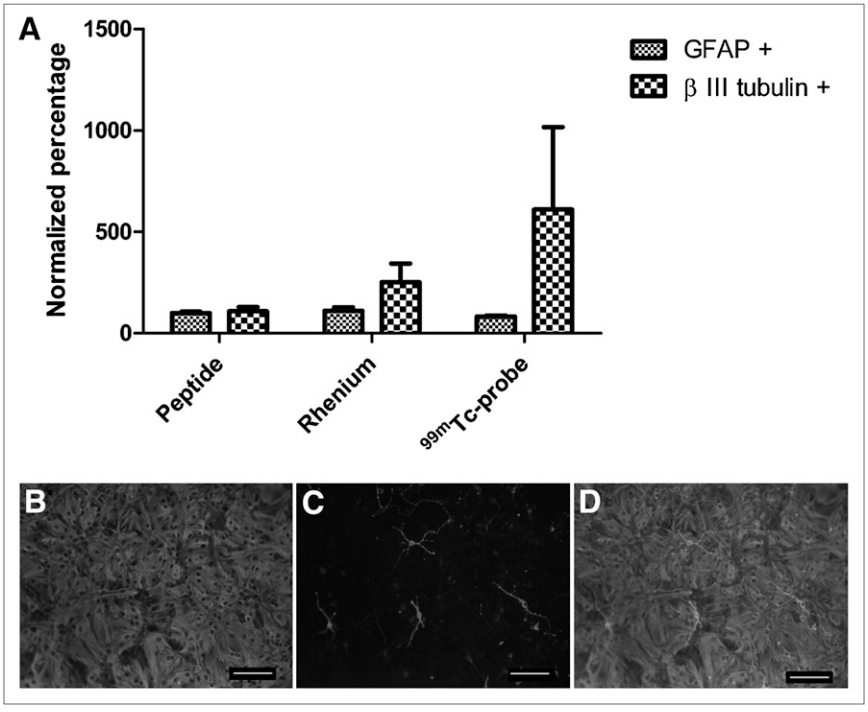


**FIGURE 2.** Differentiation profiles of NSPCs labeled with $^{99m}$Tc, rhenium, or peptide after 10 d in vitro. (A) Cells labeled with rhenium showed increased neuronal differentiation, in comparison to group of cells labeled with peptide. Highest number of neurons occurred in $^{99m}$Tc-labeled cells ($P > 0.05$, $n = 4$). (B–D) Representative differentiation image of cells labeled with glial fibrillary acidic protein (B), differentiation image of cells labeled with neuronal marker βIII-tubulin (C), and merged image (D). A color version of this figure is available as a supplemental file at http://tech.snmjournals.org.



jnmt087445-sn■ 5/7/11

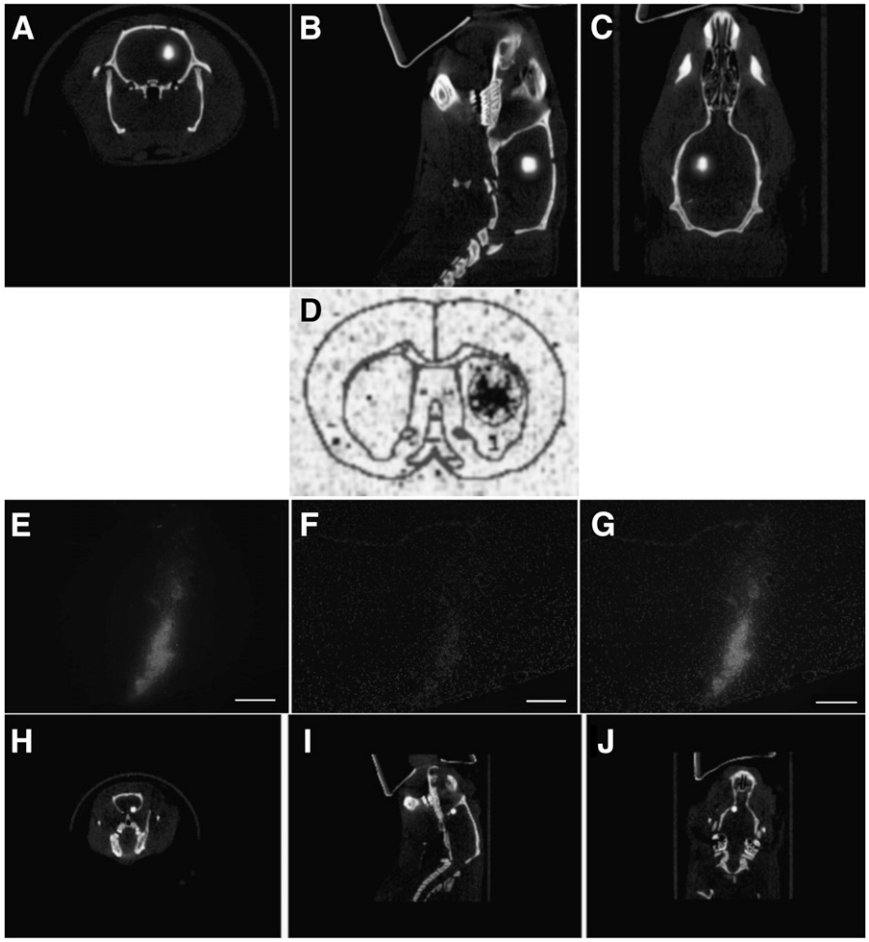


**FIGURE 3.** SPECT of unilateral transplanted NSPCs in rat. (A–C) Cells were transplanted into striatum of healthy rat and imaged with high-resolution parallel-hole SPECT/CT. There are approximately 183,000 cells in transplant site. (D) Corresponding phosphorimage of coronal section taken through transplant area. Cell transplants were also double-labeled with both $^{99m}$Tc and cell-tracker orange. (E–J) High-resolution parallel-hole SPECT/CT images were taken of cells transplanted into forebrain of animal (H–J), and coronal sections were taken for histology (E–G). Cells are shown in red and counterstained with 4′6′-diamidino-2-phenylindole. Transplant site contains approximately 16,600 cells. A color version of this figure is available as a supplemental file at http://tech.snmjournals.org.

of the number of transplantations undertaken in a typical preclinical study. An additional benefit of $^{99m}$Tc is that it imparts a low dose-burden that should limit potential radiation damage to labeled cells.

In a previous study, we developed a method to label cells for imaging after their injection into the brain (*21*). The procedure involved the use of a new chelate system, single-amino-acid chelate quinoline, which can be labeled with $^{99m}$Tc for in vivo imaging studies or with rhenium for fluorescence imaging studies. The chelate and the rhenium complex can be conveniently incorporated into peptides as if they were natural amino acids. For cell tagging, a permeation peptide, HIV $Tat_{48–57}$, was derivatized with single-amino-acid chelate quinoline or the rhenium complex, and the probes were used to label cells. Preliminary assays showed that labeling was achieved without decreasing cell viability or inducing DNA damage.

In the current study, we found a decrease in the proliferative capacity of cells labeled with $^{99m}$Tc, in comparison to rhenium- and peptide-labeled cells. This decrease may be due to radiation-induced DNA damage, which can cause cell death or arrest the cell cycle occurring outside the previously examined 24-h time point. Radiation-induced apoptosis occurs in murine lymphocytes after exposure to $^{137}$Cs. The apoptotic index peaks at 8 h, and apoptosis declines rapidly after 16 h (*23*). Because DNA damage was examined previously at 24 h, $^{99m}$Tc-induced DNA damage may have been repaired by this time or cells with irreversible damage may have been eliminated by apoptosis, as would account for the decrease in proliferation.

DNA damage caused by Auger electron emission from $^{99m}$Tc has been reported in the literature (*24–26*). Haefliger et al. (*24*) reported that DNA damage caused by the nuclear localization of $^{99m}$Tc did not reduce viability at 24 h but inhibited proliferation. At 5 d there was nuclear damage, and cell death occurred 9 d after labeling as a result of radiation-induced mitosis-linked death or radiation-induced cell senescence (*24*). The authors noted that incubation with less activity produced initial cell damage but was followed by recovery and exponential growth. For their study, cells were incubated for 36 h and the lowest concentration of peptide was in the nanomolar range, whereas our method incubated the cells for 20 min with peptide concentrations in the picomolar range. Based on the decrease in the concentration of the radiolabeled peptide and the shortened incubation in our study, it is possible that cells experienced cell-cycle arrest, slowing the proliferative capabilities of the labeled cells in comparison to the nonradioactive peptide.

DNA damage assays and apoptotic assays should be investigated further to verify DNA integrity and the viability of the $^{99m}$Tc-labeled NSPCs at later time points.

The decrease in proliferation with the present reagents may prove useful for certain cell types. For example, embryonic stem cells continue to proliferate after transplantation, potentially resulting in teratoma formation (*7*). A reduction in the proliferative capacity of these cells may result in more effective treatment with lower side effects. For cases in which a mixed population of glial cells and neurons contains an abundance of proliferating astrocytes, this probe may be advantageous to suppress the pool of dividing astrocytes. In addition, the $^{99m}$Tc probe can potentially be used to label and monitor transplants of terminally differentiated cell types for which proliferative capacity is not a concern. These avenues will require further exploration.

The differentiation of NSPCs was examined after labeling with $^{99m}$Tc, rhenium, and peptide. Although not significant, an increase in neuronal differentiation was seen when the cells were labeled with $^{99m}$Tc and rhenium. The increase in neuronal differentiation is potentially useful because neuronal differentiation in vitro is typically less common than glial differentiation (*27–29*). However, certain studies have demonstrated a pronounced neuronal differentiation of neurospheres (*30*). This finding highlights the heterogeneity of the cellular composition in neurospheres and may explain in part the variability seen in our differentiation study.

Heterogeneity within the parent spheres will likely cause heterogeneity within the differentiated population of cells, as is reflected by the fact that some reports have found a greater population of glial cells on differentiation (*29,31*) whereas other studies have found a greater population of neuronal cells (*30*). Although there is variability in the present differentiation study, the $^{99m}$Tc-labeled group consistently showed greater neuronal differentiation, suggesting that the radioactivity enhances the ability of the NSPCs to adopt a neuronal fate. This greater neuronal differentiation, in combination with the decrease in cell proliferation, may be of value for certain transplantation studies in which, typically, low numbers of neurons are seen (*32*). The mechanism by which $^{99m}$Tc favors neuronal differentiation requires further investigation.

In addition to studying the impact of the labels on cells, we compared data from SPECT/CT images after transplantation with phosphorimaging and fluorescence histology. Cell transplants were readily identified in coronal sections of the rat brain using phosphorimaging. When double-labeled with $^{99m}$Tc and cell-tracker orange, the cells could be identified by both SPECT and histology and both were localized to the same area, thereby demonstrating the accuracy of the in vivo imaging technique.

Despite attempts to repeat injections with the same number of cells into both animals, the number of implanted cells varied. We also observed this variation in our previous study, in which we attempted to perform equal bilateral transplants but found an uneven distribution of cells between the 2 transplant sites (*21*). The ability to determine the number of cells in the transplant site highlights an important benefit of labeling the NSPCs for SPECT. Previous work has shown that the number of transplanted cells affects the outcome of cell therapy. When the number of transplanted cells was varied from 25,000 to 200,000 cells/μL in a rodent model of PD, animals receiving a greater number of cells had significantly greater improvements in their functional recovery than did animals receiving a smaller graft (*14*). In addition, larger grafts contained more tyrosine hydroxylase immunoreactive neurons and enhanced the survival rate of the transplanted cells (*14*). This finding was supported by a recent study demonstrating a decrease in graft volume, cell survival, and tyrosine hydroxylase immunoreactivity in transplants when a low number of cells was injected (*13*). Larger graft volumes may stimulate the release of trophic factors and establish a better intercellular environment to increase survival and the ability to adopt a dopaminergic cell fate. Therefore, the ability to determine the number of transplanted cells may aid in predicting therapeutic outcome.

Many strategies have been undertaken to label stem cells (*33–38*); however, all these methods have been complicated by expense, lack of availability of the isotope, poor cellular uptake, or undefined biologic effects on the cells. The $^{99m}$Tc probe reported here does not compromise the integrity of the DNA or the viability of the cells at the time points we examined; however, a decrease in the proliferation of NSPCs was observed. Previous data indicate that proliferation may decrease for only the first 24 h after labeling. It will be important to determine whether the decrease in proliferation is due to radiolytic damage that is not repaired or whether proliferation is slowed because of cell cycle arrest that occurs while the cells repair the damage.

Because $^{99m}$Tc has a 6-h half-life, the monitoring of cell transplants must be done during the first 24 h. Although this timing does not allow for long-term monitoring of the cells, it does provide a method to characterize the initial transplant. Using this method, the number of cells that are successfully transplanted can be determined, and this number has been shown, in animal models, to affect therapeutic outcome (*13,14*). This determination is important to standardize the transplantation technique and enhance experimental control in preclinical and clinical settings. Such an achievement may lead to more reproducible and predictive outcomes.

## CONCLUSION

We assessed the effects of the $^{99m}$Tc probe on proliferation and differentiation of NSPCs. When the $^{99m}$Tc probe was used to monitor the cell transplants, decreases were seen in the proliferation of NSPCs in culture. However, no significant changes were found in differentiation of the cells. The accuracy of the SPECT images was validated using histochemistry and phosphorimaging. This labeling

technique allows for visualization of the transplanted cells and quantification of the number of cells within the transplant site. This information will be useful in standardizing cellular transplantations to achieve reproducible outcomes.

## ACKNOWLEDGMENT

This research was supported by the Natural Sciences and Engineering Research Council of Canada (NSERC).

## REFERENCES

1. Redmond DE Jr, Bjugstad KB, Teng YD, et al. Behavioral improvement in a primate Parkinson's model is associated with multiple homeostatic effects of human neural stem cells. *Proc Natl Acad Sci USA.* 2007;104:12175–12180.
2. Wu S, Sasaki A, Yoshimoto R, et al. Neural stem cells improve learning and memory in rats with Alzheimer's disease. *Pathobiology.* 2008;75:186–194.
3. McBride JL, Behrstock SP, Chen EY, et al. Human neural stem cell transplants improve motor function in a rat model of Huntington's disease. *J Comp Neurol.* 2004;475:211–219.
4. Zhao LR, Duan WM, Reyes M, Keene CD, Verfaillie CM, Low WC. Human bone marrow stem cells exhibit neural phenotypes and ameliorate neurological deficits after grafting into the ischemic brain of rats. *Exp Neurol.* 2002;174:11–20.
5. Klein S, Svendsen CN. Stem cells in the injured spinal cord: reducing the pain and increasing the gain. *Nat Neurosci.* 2005;8:259–260.
6. Reynolds BA, Weiss S. Generation of neurons and astrocytes from isolated cells of the adult mammalian central nervous system. *Science.* 1992;255:1707–1710.
7. Bjorklund LM, Sanchez-Pernaute R, Chung S, et al. Embryonic stem cells develop into functional dopaminergic neurons after transplantation in a Parkinson rat model. *Proc Natl Acad Sci USA.* 2002;99:2344–2349.
8. Svendsen CN, Caldwell MA, Shen J, et al. Long-term survival of human central nervous system progenitor cells transplanted into a rat model of Parkinson's disease. *Exp Neurol.* 1997;148:135–146.
9. Hahn M, Timmer M, Nikkhah G. Survival and early functional integration of dopaminergic progenitor cells following transplantation in a rat model of Parkinson's disease. *J Neurosci Res.* 2009;87:2006–2019.
10. Lindvall O, Sawle G, Widner H, et al. Evidence for long-term survival and function of dopaminergic grafts in progressive Parkinson's disease. *Ann Neurol.* 1994;35:172–180.
11. Hagell P, Schrag A, Piccini P, et al. Sequential bilateral transplantation in Parkinson's disease: effects of the second graft. *Brain.* 1999;122:1121–1132.
12. de Vries IJ, Lesterhuis WJ, Barentsz JO, et al. Magnetic resonance tracking of dendritic cells in melanoma patients for monitoring of cellular therapy. *Nat Biotechnol.* 2005;23:1407–1413.
13. Nikkhah G, Rosenthal C, Falkenstein G, Roedter A, Papazoglou A, Brandis A. Microtransplantation of dopaminergic cell suspensions: further characterization and optimization of grafting parameters. *Cell Transplant.* 2009;18:119–133.
14. Terpstra BT, Collier TJ, Marchionini DM, Levine ND, Paumier KL, Sortwell CE. Increased cell suspension concentration augments the survival rate of grafted tyrosine hydroxylase immunoreactive neurons. *J Neurosci Methods.* 2007;166:13–19.
15. Saalik P, Elmquist A, Hansen M, et al. Protein cargo delivery properties of cell-penetrating peptides: a comparative study. *Bioconjug Chem.* 2004;15:1246–1253.
16. Gammon ST, Villalobos VM, Prior JL, Sharma V, Piwnica-Worms D. Quantitative analysis of permeation peptide complexes labeled with technetium-99m: chiral and sequence-specific effects on net cell uptake. *Bioconjug Chem.* 2003;14:368–376.
17. Bhorade R, Weissleder R, Nakakoshi T, Moore A, Tung CH. Macrocyclic chelators with paramagnetic cations are internalized into mammalian cells via a HIV-tat derived membrane translocation peptide. *Bioconjug Chem.* 2000;11:301–305.
18. Lewin M, Carlesso N, Tung CH, et al. Tat peptide-derivatized magnetic nanoparticles allow in vivo tracking and recovery of progenitor cells. *Nat Biotechnol.* 2000;18:410–414.
19. Polyakov V, Sharma V, Dahlheimer JL, Pica CM, Luker GD, Piwnica-Worms D. Novel Tat-peptide chelates for direct transduction of technetium-99m and rhenium into human cells for imaging and radiotherapy. *Bioconjug Chem.* 2000;11:762–771.
20. Chianelli M, Mather SJ, Martin-Comin J, Signore A. Radiopharmaceuticals for the study of inflammatory processes: a review. *Nucl Med Commun.* 1997;18:437–455.
21. Schaffer P, Gleave JA, Lemon JA, et al. Isostructural fluorescent and radioactive probes for monitoring neural stem and progenitor cell transplants. *Nucl Med Biol.* 2008;35:159–169.
22. Ahlenius H, Visan V, Kokaia M, Lindvall O, Kokaia Z. Neural stem and progenitor cells retain their potential for proliferation and differentiation into functional neurons despite lower number in aged brain. *J Neurosci.* 2009;29:4408–4419.
23. Lemon JA, Rollo CD, McFarlane NM, Boreham DR. Radiation-induced apoptosis in mouse lymphocytes is modified by a complex dietary supplement: the effect of genotype and gender. *Mutagenesis.* 2008;23:465–472.
24. Haefliger P, Agorastos N, Renard A, Giambonini-Brugnoli G, Marty C, Alberto R. Cell uptake and radiotoxicity studies of an nuclear localization signal peptide-intercalator conjugate labeled with $[^{99m}Tc(CO)3]+$. *Bioconjug Chem.* 2005;16:582–587.
25. Pedraza-Lopez M, Ferro-Flores G, Mendiola-Cruz MT, Morales-Ramirez P. Assessment of radiation-induced DNA damage caused by the incorporation of $^{99m}Tc$-radiopharmaceuticals in murine lymphocytes using single cell gel electrophoresis. *Mutat Res.* 2000;465:139–144.
26. Ak I, Vardereli E, Durak B, et al. Labeling of mixed leukocytes with $^{99m}Tc$-HMPAO causes severe chromosomal aberrations in lymphocytes. *J Nucl Med.* 2002;43:203–206.
27. Hattiangady B, Shuai B, Cai J, Coksaygan T, Rao MS, Shetty AK. Increased dentate neurogenesis after grafting of glial restricted progenitors or neural stem cells in the aging hippocampus. *Stem Cells.* 2007;25:2104–2117.
28. Dromard C, Bartolami S, Deleyrolle L, et al. NG2 and Olig2 expression provides evidence for phenotypic deregulation of cultured central nervous system and peripheral nervous system neural precursor cells. *Stem Cells.* 2007;25:340–353.
29. Mokry J, Karbanova J, Filip S. Differentiation potential of murine neural stem cells in vitro and after transplantation. *Transplant Proc.* 2005;37:268–272.
30. Vroemen M, Aigner L, Winkler J, Weidner N. Adult neural progenitor cell grafts survive after acute spinal cord injury and integrate along axonal pathways. *Eur J Neurosci.* 2003;18:743–751.
31. Ader M, Schachner M, Bartsch U. Integration and differentiation of neural stem cells after transplantation into the dysmyelinated central nervous system of adult mice. *Eur J Neurosci.* 2004;20:1205–1210.
32. Muraoka K, Shingo T, Yasuhara T, et al. Comparison of the therapeutic potential of adult and embryonic neural precursor cells in a rat model of Parkinson disease. *J Neurosurg.* 2008;108:149–159.
33. Zhou R, Thomas DH, Qiao H, et al. In vivo detection of stem cells grafted in infarcted rat myocardium. *J Nucl Med.* 2005;46:816–822.
34. Ma B, Hankenson KD, Dennis JE, Caplan AI, Goldstein SA, Kilbourn MR. A simple method for stem cell labeling with fluorine 18. *Nucl Med Biol.* 2005;32:701–705.
35. Bai J, Ding W, Yu M, et al. Radionuclide imaging of mesenchymal stem cells transplanted into spinal cord. *Neuroreport.* 2004;15:1117–1120.
36. Chin BB, Nakamoto Y, Bulte JW, Pittenger MF, Wahl R, Kraitchman DL. $^{111}In$ oxine labelled mesenchymal stem cell SPECT after intravenous administration in myocardial infarction. *Nucl Med Commun.* 2003;24:1149–1154.
37. Aicher A, Brenner W, Zuhayra M, et al. Assessment of the tissue distribution of transplanted human endothelial progenitor cells by radioactive labeling. *Circulation.* 2003;107:2134–2139.
38. Ford JW, Welling TH III, Stanley JC, Messina LM. PKH26 and $^{125}I$-PKH95: characterization and efficacy as labels for in vitro and in vivo endothelial cell localization and tracking. *J Surg Res.* 1996;62:23–28.